8-2001

Sensitivity of simulated regional surface thermal fluxes during warm advection snowmelt to selection of the lowest model level height

H. Wei
Iowa State University

Moti Segal
Iowa State University, segal@iastate.edu

William J. Gutowski Jr.
Iowa State University, gutowski@iastate.edu

Z. Pan
Iowa State University

Raymond W. Arritt
Iowa State University, rwarritt@iastate.edu

See next page for additional authors

Authors
H. Wei, Moti Segal, William J. Gutowski Jr., Z. Pan, Raymond W. Arritt, and William A. Gallus Jr.

Sensitivity of Simulated Regional Surface Thermal Fluxes during Warm Advection Snowmelt to Selection of the Lowest Model Level Height

H. WEI,*,+ M. SEGAL,# W. J. GUTOWSKI JR.,*,# Z. PAN,# R. W. ARRITT,# AND W. A. GALLUS JR.*

*Department of Geological and Atmospheric Science, Iowa State University, Ames, Iowa
#Department of Agronomy, Iowa State University, Ames, Iowa

(Manuscript received 16 November 2000, in final form 6 April 2001)

ABSTRACT

Under strong warm advection, sensible and latent heat fluxes may provide larger energy for surface snowmelt than does net radiation flux. With these thermally stable conditions, the height of the first model level may be well above the surface-layer depth and thus outside the range of applicability of the surface-layer similarity theory on which the models' surface thermal flux computation is based. This situation can strongly affect the magnitude of simulated surface thermal fluxes and snowmelt. To explore this issue, the impact of selected heights of the first model level on the simulated surface fluxes and snowmelt under stable surface stratification conditions was investigated. Simulations using a mesoscale atmospheric model considering two extreme contrasts in surface roughness were performed. Setting the first model level to 3 or 10 m, which typically was within the stable surface layer, yielded nearly the same contribution of simulated surface turbulent thermal fluxes to snowmelt. When the first model level height was set at about 40 m, as is used in many regional model simulations, it exceeded the depth of the stable surface layer over the snow cover. The surface turbulent thermal flux contribution in this case was smaller (by about 40%), with a directly proportional effect on the snowmelt. Pending observational support, results presented in this study imply that setting a model's lowest level to 10 m or less will likely improve simulated snowmelt accuracy during warm advection.

1. Introduction

In many warm advection situations, the main energy source for snowmelt is downward sensible and latent heat fluxes from the atmosphere, particularly during the nighttime or under cloudy daytime conditions. Accurate simulation of these fluxes in coupled atmosphere–snow models has, therefore, a significant influence on snowmelt in such situations. Atmospheric models use surface-layer similarity formulation to calculate the surface thermal fluxes based on surface winds, temperature, and humidity. Implicitly, therefore, it is assumed in these models that the lowest level is within the surface layer where the similarity theory holds. The surface-layer depth is considered to be the layer in which the momentum and thermal fluxes are approximately constant. For scaling purposes, however, the surface-layer depth is commonly defined as the depth within which the variation in the momentum flux is less than or equal to 10% (e.g., Panofsky and Dutton 1984). The surface-layer depth typically ranges from a few meters for very stable thermal stratification to a few tens of meters for slightly stable stratification; for unstable thermal stratification, its height is several tens of meters to about 100 m. Therefore, in model simulations, the computed sensible and latent heat fluxes may be sensitive to the selection of the first model level relative to the surface-layer depth. However, in many reported regional atmospheric model simulations (e.g., Takle et al. 1999), the selected first model levels probably are well above the top of the stable surface layer. If the lowest model level is higher than the surface-layer depth, the surface-layer formulation is applied where the assumptions used in its derivation may be no longer valid. Inappropriate selection of the first model height relative to the surface-layer height may lead, therefore, to noticeable errors in surface fluxes.

In general circulation models (GCMs) and regional models, the first model level above the earth's surface is frequently set at a height of several tens of meters or greater. Although the first model level might be within the unstable surface layer, it would tend to be above the surface layer under stable surface-layer conditions. One might expect that under unstable surface stratification over snow-free land during the daytime, when the surface layer is relatively deep, the first model level even if relatively high would tend to be within the surface

+ Current affiliation: Polar Meteorology Group, Byrd Polar Research Center, The Ohio State University, Columbus, Ohio.

Corresponding author address: Moti Segal, Department of Agronomy, 3010 Agronomy Hall, Iowa State University, Ames, IA 50011.
E-mail: segal@iastate.edu

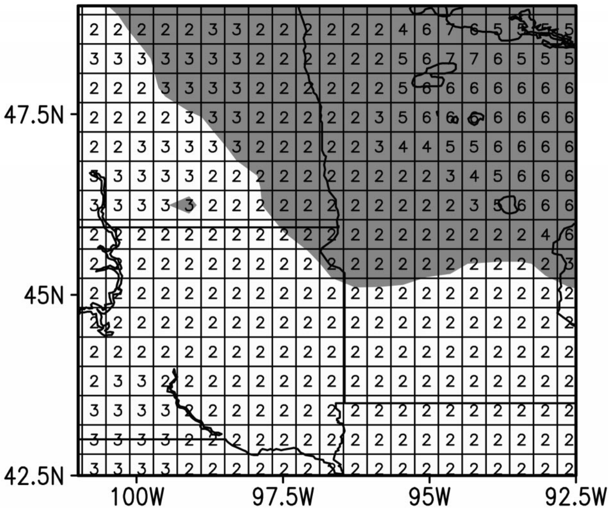

FIG. 1. The land use types in the study area (see text for explanation). The locations with initial snow cover are shaded.

layer. Thus any potential bias in the computed sensible heat flux is likely to be relatively small in response to the height selection of the first model level. In contrast, under nocturnal stable conditions over snow-free land the *relative* bias in sensible heat flux may be large when the first model level is considerably higher than the surface-layer height. However, in this situation the value of the sensible heat flux is typically 1 order of magnitude lower than that for daytime conditions, so the impact of sensible heat flux bias on predicted lower-atmosphere meteorological fields would tend to be at most moderate. Under strong warm-advection conditions over an area experiencing snowmelt, the surface layer is always stable and its thermal stability strength is only moderately affected by wind speed, because the snow skin temperature cannot exceed 273.16 K. (Over bare soil, the skin temperature increases somewhat with wind speed in stable situations, reducing the thermal stability of the surface layer.) Therefore, unlike the stable nocturnal surface layer over bare soil, downward surface sensible and latent heat fluxes over snow cover may be high under warm-advection conditions. Sensible and latent heat fluxes of several hundred watts per square meter can occur under these conditions (e.g., Cline 1997; Leathers et al. 1998; Segal et al. 1991). In this situation, selecting a first model level above the surface layer may reduce the surface turbulent heat fluxes considerably, leading to underprediction of snowmelt. The radiative and substrate thermal fluxes are likely to be marginally sensitive to the first model level height.

The increased use of coupled snow–atmosphere regional models for snowmelt prediction suggests that evaluation of the sensitivity of surface turbulent thermal fluxes to the selection of first model level height would be beneficial. This study addresses this issue by (i) a conceptual scaling evaluation that suggests constraints on the surface layer's maximum depth and (ii) case-study sensitivity simulations with the first model level set at about 3, 10, and 40 m to evaluate the effects of surface-layer resolution on surface turbulent thermal fluxes and snowmelt. The surface turbulent thermal fluxes in the case of warm advection over snow are also sensitive to the selection of the surface roughness parameter. To address this issue, the model simulations were carried out for two contrasting extreme snow cover surface roughness conditions.

2. General scaling evaluation

In the following, we present several concepts that are used later with regional numerical model simulations to evaluate how warm advection over snow cover constrains selection of the first model level.

a. Constraints on the stable surface-layer depth based on similarity relations

In Monin–Obukhov similarity theory, the nondimensional wind shear within the surface layer is given by

$$\frac{kz}{u_*}\frac{\partial \overline{u}}{\partial z} = \phi_m, \tag{1}$$

where k ($\cong$0.4) is the von Kármán constant, z is height, u_* is the friction velocity, and $\overline{u}$ is the wind speed. The rhs of (1) can be expressed for the stable surface layer as

$$\phi_m = 1 + \beta\xi, \tag{2}$$

where β is a constant and $\xi = z/L$. Here, L is the Monin–Obukhov length [$L = (\theta\rho c_p u_*^3)/(kgH_s)$], where θ is the background potential temperature; ρ and c_p are the air density and specific heat, respectively; g is the gravity acceleration; and H_s is the surface sensible heat flux. Skibin and Businger (1985) surveyed earlier observational studies and concluded that for stable stratification (2) holds for $z/L \leq 1$. In analysis of observations from the Kansas, Moses Lake (Washington), and Wangara (Australia) field experiments, they reaffirmed that (2) represents the velocity profile close to the ground in stable stratification (with $\beta = 4.7$) up to $z/L \cong 1$. Skibin and Businger (1985) also found that (2) might hold somewhat above the surface layer, that is, extending to a portion of the stable boundary layer. The above results suggest that $h_s \leq L$, where h_s is the depth of the surface layer. This relation implies that in model simulations the commonly used similarity-based formulation to compute the surface layer fluxes imposes the constraint $z_1 < L$, where z_1 is the first model level height. However, this evaluation does not tell us how much lower than L the value of z_1 needs to be. In a physical sense, L reflects the height at which mechanical generation of turbulence is offset by negative buoyant production by the stable stratification. One would anticipate a drop in the momentum flux above this height and possibly even at lower heights, consistent with the suggested constraint $h_s \leq L$.

b. Formulation for computing simulated surface-layer depth

In the following we evaluate the depth of the surface layer, indicating the maximum possible z_1 in the model simulations to resolve appropriately the sensible and latent heat fluxes.

The steady-state equation for horizontal momentum in the surface layer can be written approximately as

$$\frac{1}{\rho}\frac{\partial \boldsymbol{\tau}}{\partial z} - f\mathbf{k} \times \mathbf{v} + f\mathbf{k} \times \mathbf{v}_g = 0, \quad (3)$$

where $\boldsymbol{\tau}$ is the eddy stress, f is the Coriolis parameter, $\mathbf{v}$ and $\mathbf{v}_g$ are the wind velocity and the geostrophic wind velocity in the surface layer, respectively, and $\mathbf{k}$ is the unit vector in the vertical direction. Within the surface layer $\mathbf{v}_g$, $\mathbf{v}$, and $\boldsymbol{\tau}$ approximately do not change direction; thus, integrating (3) from the surface to the top of the surface layer yields

$$\tau_0 - \tau_{h_s} = f\int_0^{h_s} \rho|\mathbf{v}_g - \mathbf{v}|\, dz, \quad (4)$$

where h_s is now the height of the surface layer top, τ_0 is the surface stress, and τ_{h_s} is the stress at the top of the surface layer.

Because the surface-layer depth is defined as the layer in which the surface eddy stress changes by less than or equal to 10%, (4) can be written as

$$\frac{\tau_0 - \tau_{h_s}}{\tau_0} = 0.1 = \frac{f\rho|\mathbf{v}_g - \overline{\mathbf{v}}|h_s}{\tau_0}, \quad (5)$$

where $\overline{\mathbf{v}}$ is the average of $\mathbf{v}$ within the surface layer. Using the relation $\tau_0 = \rho u_*^2$, we obtain from (5),

$$h_s = \frac{0.1u_*^2}{f|\mathbf{v}_g - \overline{\mathbf{v}}|}. \quad (6)$$

One would anticipate under a stable boundary layer situation that there would be a relatively rapid drop in the momentum flux above h_s, with the flux ultimately dropping to zero at the top of the boundary layer. If $z_1 \le h_s$, then the vertical turbulent flux computed by the model at z_1 should be a good approximation to the magnitude of the flux at the surface. If instead, $z_1 > h_s$, then the flux computed by the model can differ from the flux at the surface. Because fluxes will tend to decrease with height from the top of the surface layer to the top of the stable boundary layer, when $z_1 > h_s$, the erroneous assumption that z_1 is in the surface (constant flux) layer will likely result in a surface flux weaker in magnitude than it should be.

For computational simplicity we define h_s^1 as

$$h_s^1 = \frac{0.1u_*^2}{f|\mathbf{v}_g - \overline{\mathbf{v}}_1|}, \quad (7)$$

where $\overline{\mathbf{v}}_1$ is the average wind velocity within the first model layer (approximated as $0.5|\mathbf{v}_1|$). In the surface layer, the wind speed increases with height; therefore, $|\overline{\mathbf{v}}_1| \le |\overline{\mathbf{v}}|$, and comparing (6) and (7) implies $h_s^1 \le h_s$. Satisfying the constraint $z_1 \le h_s^1$ would therefore imply an appropriate selection of z_1 relative to the surface-layer depth. In addition, however, in numerical models the application of surface-layer similarity functional relations is confined to the first model layer. Consistency with this modeling constraint requires imposing $z_1 \le h_s^1$.

3. Model evaluations

a. Brief description of the model

The model adopted in this study is a nonhydrostatic version of the Fifth-Generation Pennsylvania State University–National Center for Atmospheric Research (NCAR) Mesoscale Model (MM5), which is widely used for meteorological research and short-term weather forecasting. The model uses a terrain-following σ coordinate in the vertical. The model physics includes a revised version of Blackadar's planetary boundary layer model (Zhang and Anthes 1982), which is used to predict surface layer and boundary layer properties. An explicit treatment of cloud water, rainwater, snow, and ice (Dudhia 1989) and a cumulus convective scheme (Grell 1993) are used for precipitation physics. Radiative transfer follows the method of Dudhia (1989). A detailed description of MM5 appears in Grell et al. (1995).

In this study, we used the original surface-layer formulation of MM5 together with a simplified approach for modeling snowmelt. A slab snow module was incorporated into MM5, using the surface energy balance equation

$$\rho_s C_s S_{\rm we}\frac{\partial T_s}{\partial t} = R_n - H_s - H_l - H_g - H_r - H_f. \quad (8)$$

The equation predicts snow-layer temperature T_s, where ρ_s is snow density, C_s is the specific heat of ice, and $S_{\rm we}$ is snow water equivalent. The energy budget equation includes net surface radiation R_n, sensible heat flux H_s, latent heat flux H_l, heat flux from substrate H_g, melting heat from falling rain H_r, and heat H_f released when rain freezes on the surface. We use the sign convention that nonradiative fluxes are positive away from the surface and radiative fluxes are positive toward the surface. If T_s is greater than 273.16 K, the snowmelt in a time step is calculated by

$$\Delta S_{\rm we} = C_s S_{\rm we}(T_s - 273.16)/L_i, \quad (9)$$

where L_i is the latent heat of ice fusion. Precipitation is assumed to be snow when air temperature in the lowest model level is below 273.16 K. A multilayer soil model is used below the snow layer.

b. Simulation setting

We used the fast-snowmelt episode during April of 1997 in the north-central United States (Cline and Carroll, 1999) to study the impact of z_1 selection on snow surface thermal fluxes. The simulation period was 0000 UTC 4 April–0000 UTC 6 April 1997. The model domain consisted of 101 $\times$ 75 horizontal grid points covering most of the United States with 45-km grid spacing. We focused our analyses on a subdomain illustrated in Fig. 1, which was covered by snow in its northern portion. The land use types in Fig. 1 and the corresponding surface roughness parameter (in parentheses) are: 2, agricultural land (5 cm); 3, range grassland (10 cm); 4, deciduous forest (50 cm); 5, coniferous forest (50 cm); 6, mixed forest and wetland (40 cm); and 7, water (roughness parameter computed by the model). The vegetation types in the domain of interest are based on MM5's standard land use database for winter. A stationary front extended from northern Minnesota into western South Dakota (located at the convergence zone of the surface flow presented in Fig. 2). Intense snowmelt occurred during the simulation period in the warm sector of the front.

Meteorological initial and lateral boundary conditions (wind components, temperature, water vapor mixing ratio, and surface pressure) necessary to drive the model runs were interpolated from the surface and sigma-level data of the National Centers for Environmental Prediction–NCAR reanalysis (Kalnay et al. 1996). The lateral boundary conditions were updated every 6 h with relaxation boundary conditions. The initial snow water equivalent (SWE) in the analysis domain was interpolated from the observation-driven model results reported in Cline and Carroll (1999). Observations from the National Weather Service were used to initialize the SWE field outside the analysis domain.

Two simulations were performed using contrasting extremes for the snow surface roughness parameter. (i) ''Rough surface simulation'' is a simulation in which the roughness parameter was prescribed as that of the canopy for grid points with snow cover and vegetative canopy (occasionally, following snowfall on vegetation such as conifers or shrubs, the canopy is covered with snow for some period, so that the surface roughness parameter resembles that of the snow-free vegetation). (ii) In the ''smooth surface simulation,'' it was assumed that all grid points with snow cover were canopy free. A surface roughness parameter of 0.4 cm was adopted at these grid points, following the survey for roughness parameters over melting snow reported in Moore (1983). For both cases we performed three model runs, with the

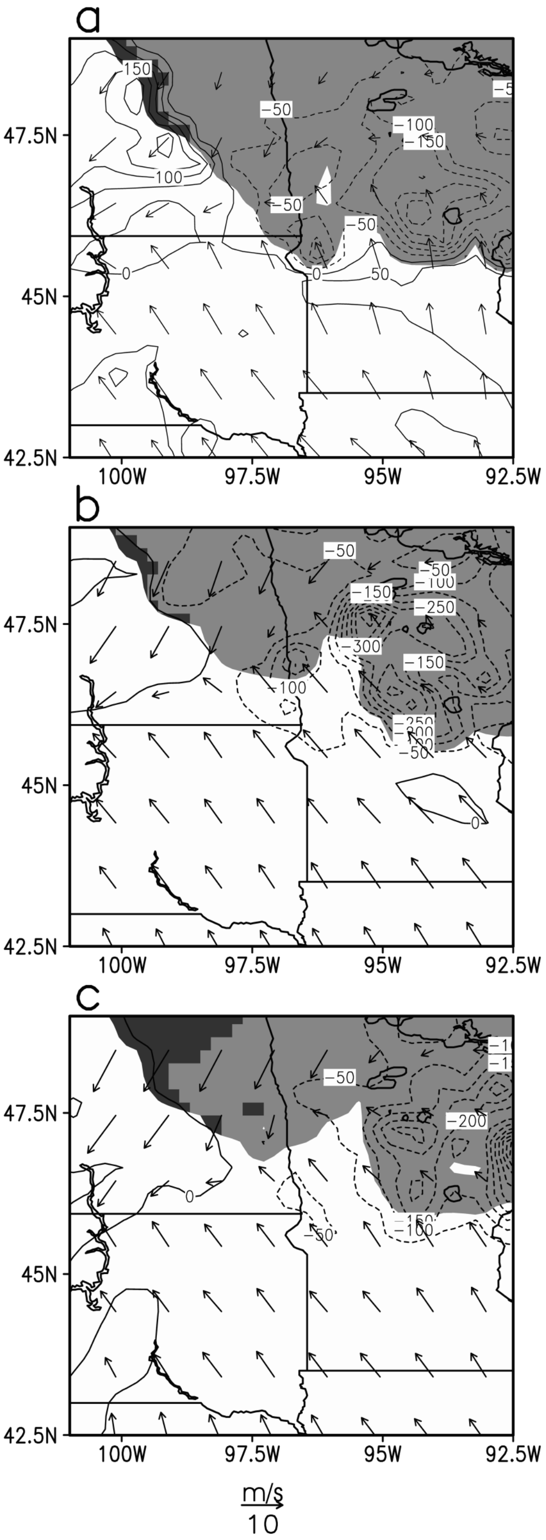

←

FIG. 2. Simulated sensible heat flux (W m^{-2}; positive away from the surface) and wind velocity at the first model level ($\mathbf{v}_1$) in exp3R for three individual hours during 4–5 Apr 1997: (a) 1800 UTC 4 Apr, (b) 0000 UTC 5 Apr, and (c) 0600 UTC 5 Apr. Contour interval is 50 W m^{-2}, with wind vector scale (m s^{-1}) shown at bottom. Snow-covered areas with a thermally stable surface layer are shaded lightly; dark shading indicates snow cover associated with an unstable surface layer.

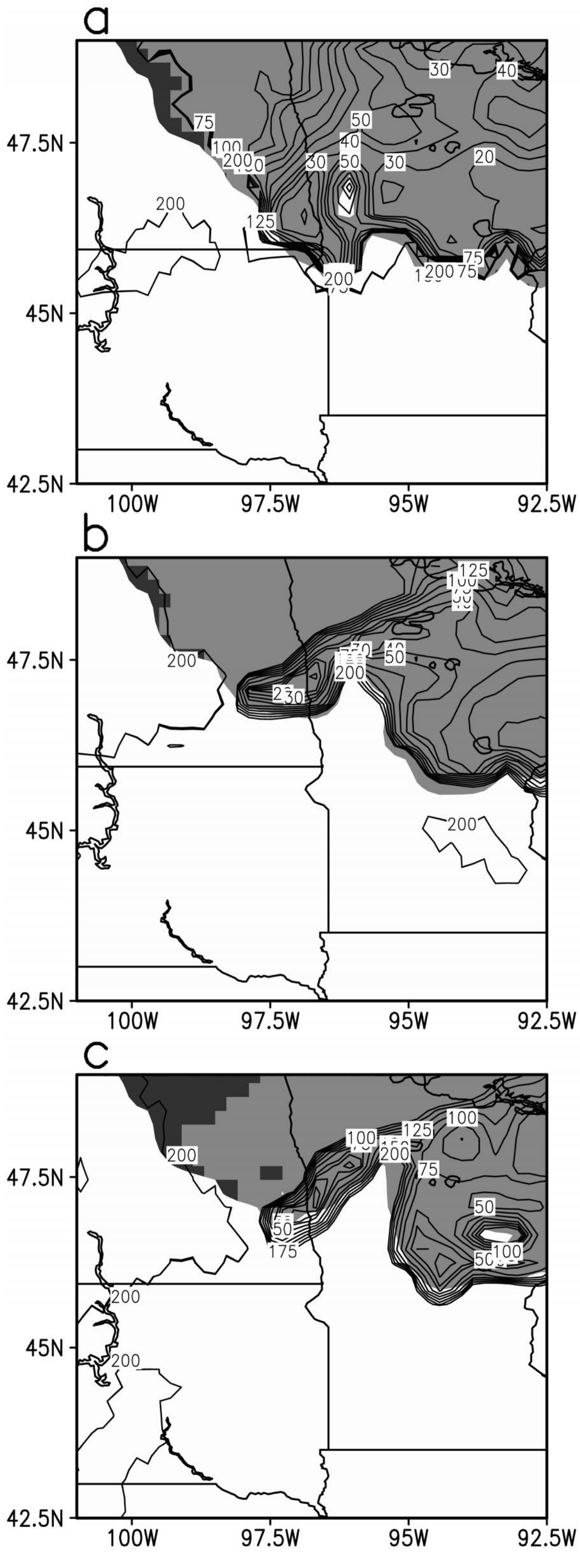

FIG. 3. Simulated Monin–Obukhov length L (m) in exp3R for three individual hours during 4–5 Apr 1997: (a) 1800 UTC 4 Apr, (b) 0000 UTC 5 Apr, and (c) 0600 UTC 5 Apr. Contours are shown only for locations where $0 \leq L < 200$ m. Contour interval is 10 m when $L < 50$ m and 25 m when $L \geq 50$ m.

first model level height z_1 at about 3, 10, and 40 m (denoted exp3R, exp10R, and exp40R, respectively, for the rough surface simulation case and exp3S, exp10S, and exp40S for the smooth surface simulation case). Note that the model uses a sigma coordinate so that the specified z_1 values are approximations. We estimate that, in the simulated domain, the values of z_1 can vary from the values stated above by $\pm 2\%$.

The main objectives of the simulations were (i) to evaluate whether the first model level is low enough over the analysis domain to resolve appropriately the surface layer's characteristics and (ii) to evaluate the impact of selecting higher first model levels on the simulated sensible and latent heat fluxes.

4. Simulation results

a. Rough surface simulation

1) SIMULATED H_s, $\mathbf{v}_1$, AND L

Figure 2 presents the H_s and $\mathbf{v}_1$ fields at three selected hours for exp3R. The snow-covered area associated with a stable surface layer (i.e., the snow affected by warm advection) is lightly shaded. The snow area associated with an unstable surface layer is shaded with a darker color (this area is not of interest for these evaluations). A portion of the snow-covered area was affected by intense downward H_s due to relatively strong wind advecting warm air from the south. The peak magnitude for H_s over the snow area reached a few hundred watts per square meter. In some newly formed snow-free strips juxtaposed to the snow-cover edge, the soil layer was a strong thermal sink, thus supporting relatively high values of downward sensible heat fluxes. It is interesting to note the increased upward sensible heat flux behind the stationary front during the daytime (Fig. 2a), supported in part by advection of cold air from the snow-covered area toward the bare soil area. In the southern half of the domain, where snow cover is absent, the sensible heat flux is low because of cloudiness. Simulated patterns of the H_l fields resembled those described for H_s but with characteristically lower values.

Exp3R allows us to evaluate the constraint $z_1 \leq L$, outlined in section 2a. In this simulation, the first model level at 3 m is presumed to be within the surface layer. The simulated L fields for three selected hours appear in Fig. 3. The range of the plotted L values is 10–200 m, showing that for $z_1 = 3$ m the constraint $z_1 \leq L$ prevails. However, the simulated L fields suggest that when $z_1 = 40$ m the constraint $z_1 \leq L$ will be violated in some portion of the snow-covered area for the two earlier hours (Figs. 3a,b) but not in the last hour presented (Fig. 3c). Based on the discussion in section 2a, the results imply that $z_1 = 40$ m is too high for the first model level, at least for a portion of the simulation's area and period. We also computed L fields for exp40R (not shown). In that case, $L < 40$ m (implying $z_1 \geq L$)

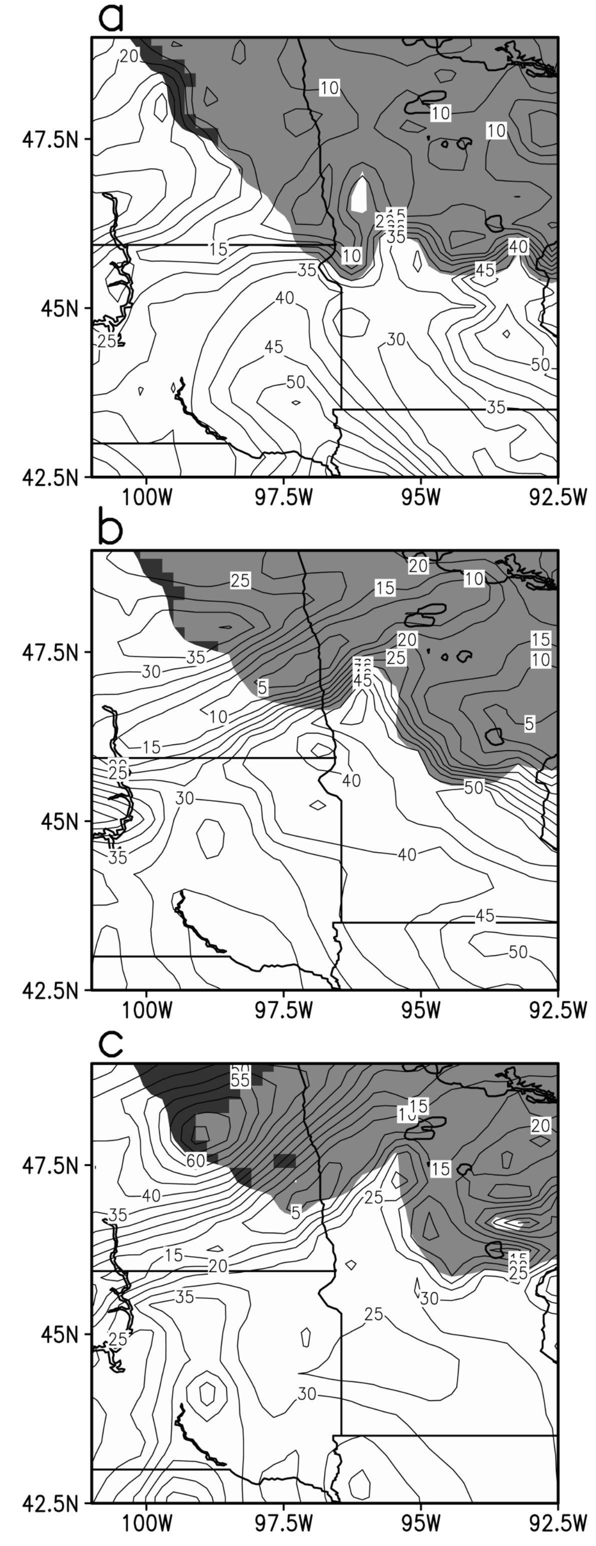

FIG. 4. Simulated h_s^1 (m) in exp3R for three individual hours during 4–5 Apr 1997: (a) 1800 UTC 4 Apr, (b) 0000 UTC 5 Apr, and (c) 0600 UTC 5 Apr. Contour interval is 5 m.

over an even wider area when compared with that in exp3R.

2) Simulated h_s^1

Figure 4 presents the h_s^1 for three different hours in exp3R using (7) and model-simulated values of the variables for the period with very rapid snowmelt. The snow skin temperature was typically 0°C. At 1800 UTC 4 April (Fig. 4a), the simulated values of h_s^1 over the snow area were mostly in the range 5–25 m. A larger range of values is simulated at 0000 UTC 5 April (Fig. 4b). Over the snow-free areas, h_s^1 values in both hours were higher than over the snow area, peaking at about 50 m. The increased h_s^1 values reflect increased wind speed (see Fig. 2) and reduced thermal stability of the surface layer over the snow-free areas. Around midnight (0600 UTC 5 April; Fig. 4c), low h_s^1 values over the central sector of the snow cover persist as the skin temperature was constrained to 0°C. Note that low values of h_s^1 are associated with a flow convergence zone related to the stationary front located in the northwest sector of the domain (see Fig. 2). Comparing Fig. 4 and Fig. 2, one can see that in snow areas affected by strong downward sensible heat flux, the h_s^1 values were in the range of 5–25 m, implying a need for a relatively low z_1 to resolve appropriately the surface sensible heat flux. Figure 5 presents the computed h_s^1 fields in exp40R. Over the snow-covered area affected by warm advection, typically h_s^1 is less than 40 m; thus, the requirement that z_1 must be within the surface layer is likely violated.

3) Sensitivity of H_s to the selection of z_1

Figure 6 presents a time series of H_s averaged over the snow area for the three rough simulations. The H_s averages were computed for the whole snow-covered area (Fig. 6a) and for subregions classified by thermal stability (Figs. 6b–d). In Fig. 6b only those grid points with $T_1 > 1$°C were used in the average (T_1 is the air temperature at the first model level), and in Fig. 6c and Fig. 6d only points with $T_1 > 3$°C and $T_1 > 5$°C, respectively, were used. The difference in H_s is relatively small between exp3R and exp10R, both of which had the first model level over snow within the surface layer. However, H_s in exp40R is generally much smaller than in the other two cases during the whole simulation. The largest difference when comparing exp40R with exp10R and exp3R is found around sunset on 5 April when surface-layer stratification over the snow cover was the most thermally stable of the day because of enhanced warm advection. Note that for exp40R the first model level height z_1 was implied to be typically higher than the surface layer, and thus the similarity theory's applicability is compromised. Last, evaluations as described above were carried out for the surface latent heat flux H_l. Similar patterns were indicated; however,

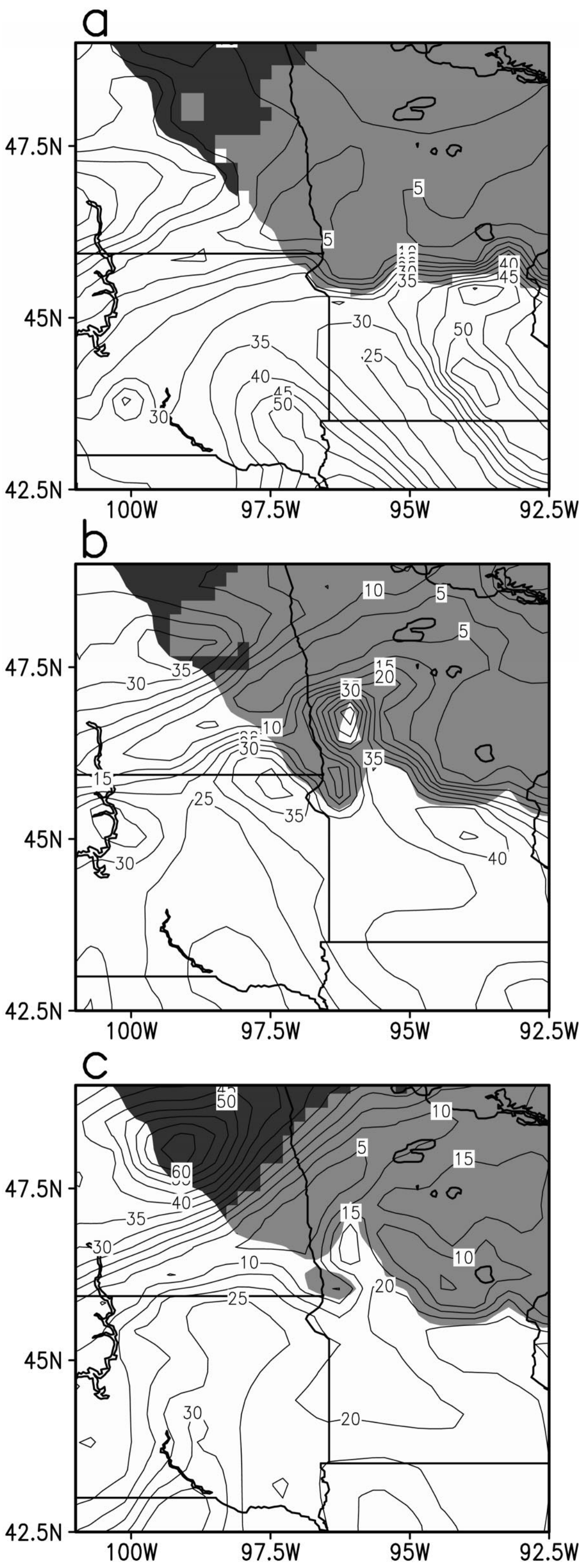

FIG. 5. As in Fig. 4, but for exp40R.

the characteristic magnitudes of H_l were at most one-half of those simulated for H_s (not shown).

b. *Smooth surface simulation*

Three simulations were carried out: exp3S, exp10S, and exp40S, which are the same as exp3R, exp10R, and exp40R, respectively, except that the surface roughness parameter is 0.4 cm for snow grid points. These simulations provide an extreme contrast to the rough snow surface simulation described previously. The simulated fields for L and h_s^1 in general resembled those presented in section 4a for the rough surface simulation, suggesting the same constraints on the height of the lowest model level. Heights of 3 and 10 m for the first model level typically were within the surface layer, whereas the 40-m model level likely was above the surface layer (not shown).

Because of the low surface roughness, sensible heat flux into the snow cover (Fig. 7) was less than in the corresponding rough surface simulations (Fig. 2). Also, the surface wind speed increased noticeably in response to the reduced surface roughness parameter. The distribution of the sensible heat flux over the snow resembled that presented in Fig. 1; however, its peak values were noticeably smaller.

Figure 8 presents time series of H_s averaged over the snow area for the three simulated cases exp3S, exp10S, and exp40S. The magnitude of the averaged H_s was smaller in this set of experiments when compared with the rough surface simulation (Fig. 6); however, its temporal variation was similar to that in the rough case. Also, in this case as in the rough surface case, the magnitude of H_s for simulations with a first model level at 3 and 10 m tended to be similar, whereas the magnitude of H_s for $z_1 = 40$ m was noticeably lower. The results suggest that, for the low–surface roughness simulation, too, a first model level above the surface layer over snow cover results in underestimated surface sensible heat flux. A similar result was apparent for the latent heat flux patterns (not shown). Last, note that the actual sensible heat flux values will probably be somewhere between those obtained in the limiting cases (rough and smooth) presented here.

c. *Sensitivity of simulated snowmelt to the selection of z_1*

In both simulations (the rough and the smooth snow surface) the sensible heat flux was the major thermal forcing for snowmelt, and the contribution from latent heat flux was secondary (in the average for all simulations $H_l/H_s \cong 0.3$). Both fluxes were sensitive to the height of z_1 as evaluated in previous subsections. The other surface thermal fluxes, including the net radiation, the heat flux from the substrate, and rainfall-related heat sources (H_r and H_f), were affected negligibly by the changes in z_1. Thus, the change in SWE during the

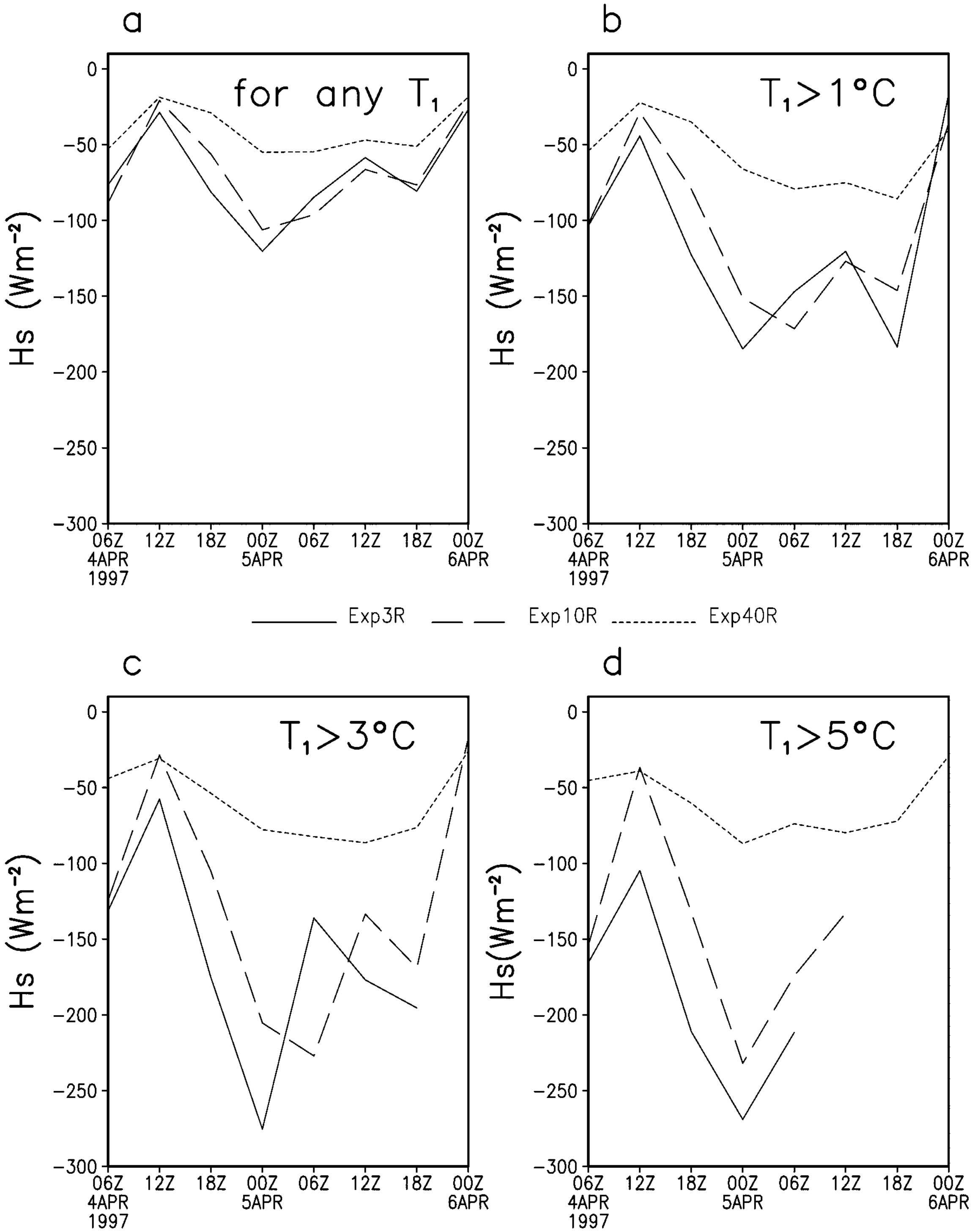

FIG. 6. Time series for 4–5 Apr 1997 of domain-averaged sensible heat flux over the snow-covered area in exp3R, exp10R, and exp40R: (a) over all snow-covered grid points, (b) over snow-covered grid points with $T_1 > 1°C$, (c) as in (b) but for $T_1 > 3°C$, and (d) as in (b) but for $T_1 > 5°C$ (T_1 is the air temperature at the first model level).

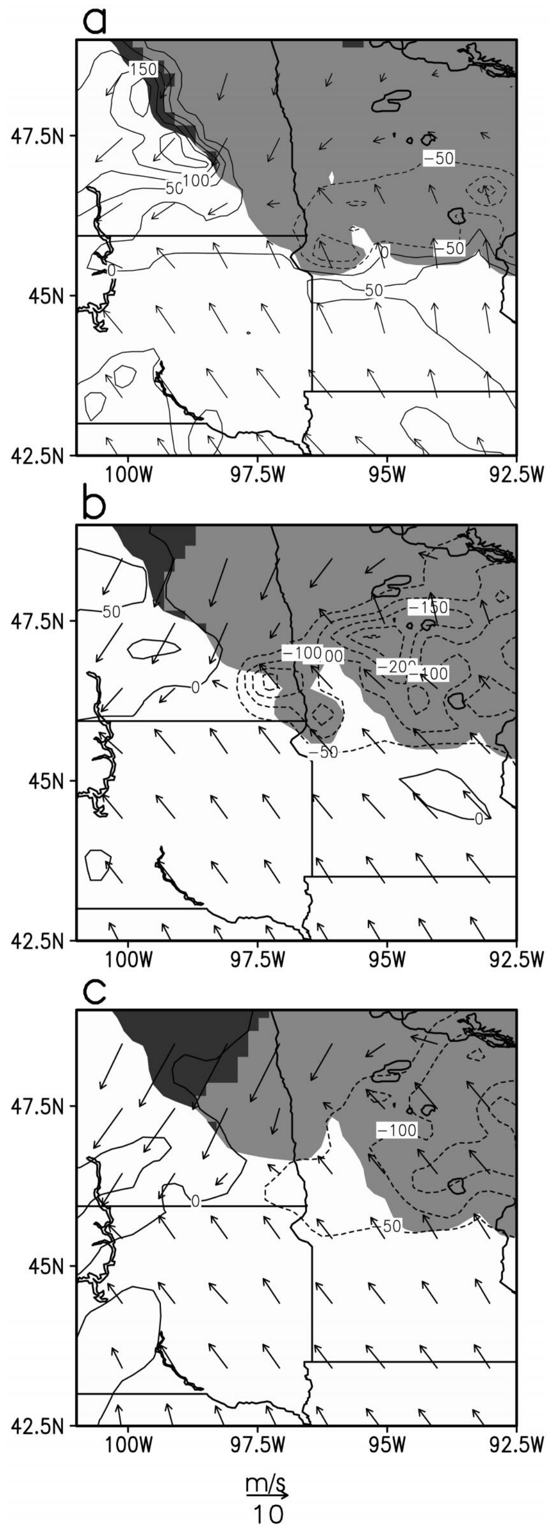

FIG. 7. As in Fig. 2, but for exp3S.

48-h simulation period would be sensitive to changes in z_1 only in response to variations in surface moist enthalpy flux ($H_s + H_l$).

Figure 9 presents the change in SWE summed (not averaged) over all initially snow-covered grid points during the simulation period, in response to variations in z_1 (the initial total SWE in the domain was 1130 cm). For the rough surface simulations, the change in SWE was almost identical for exp3R and exp10R; however, it dropped by approximately 30% in exp40R [note also the smaller extent of snow cover in exp3R (Fig. 2c) as compared with that in exp40R (Fig. 5c)]. The average sum of the sensible and latent heat flux for the snow-covered domain was about 40% lower in exp40R as compared with exp3R and exp10R. Likewise for the smooth surface simulation the change in SWE was closely similar for exp3S and exp10S, but with somewhat lower values in comparison with exp3R and exp10R, respectively. The drop in the change of SWE and of the sum of latent and sensible heat flux computed in exp40S resembled that stated above for the rough surface simulations. Overall, for the presented case study the domain-accumulated snowmelt is sensitive to the selection of z_1. This sensitivity was even more pronounced when focusing only on the period of very intense warm advection and surface moist enthalpy fluxes during 1800 UTC 4 April–0600 UTC 5 April 1997.

5. Summary

We have examined how the choice of the lowest model level affects surface heat fluxes and snowmelt under strong warm advection. It is found that surface heat fluxes, particularly sensible heat flux, are sensitive to the height of the first model level. During warm advection situations, these fluxes may be the main energy source for snowmelt. Because the surface thermal stratification over the snow-covered area is stable under warm advection conditions, the surface layer tends to be relatively shallow. Regional model sensitivity simulations for two contrasting extreme surface roughness parameters showed that, for the first model level at 3 or 10 m, similar sensible heat fluxes result over the snow area, because the first model level in both cases is within the stable surface layer. In the simulated case with the first model level at 40 m, representative of values often used in regional simulation studies, the average sum of the sensible and latent heat flux for the snow-covered domain was about 40% lower as compared with the 3- and 10-m first level simulations. In this simulation, the first model level was diagnosed as above the surface layer over a large number of snow-covered grid points, resulting in a bias in simulating these thermal fluxes. This bias led to about a 30% underestimate of snowmelt as compared with the other two cases. Pending observational support, results presented in this study imply that setting a model's lowest level to 10 m or less will likely increase the magnitude of snowmelt.

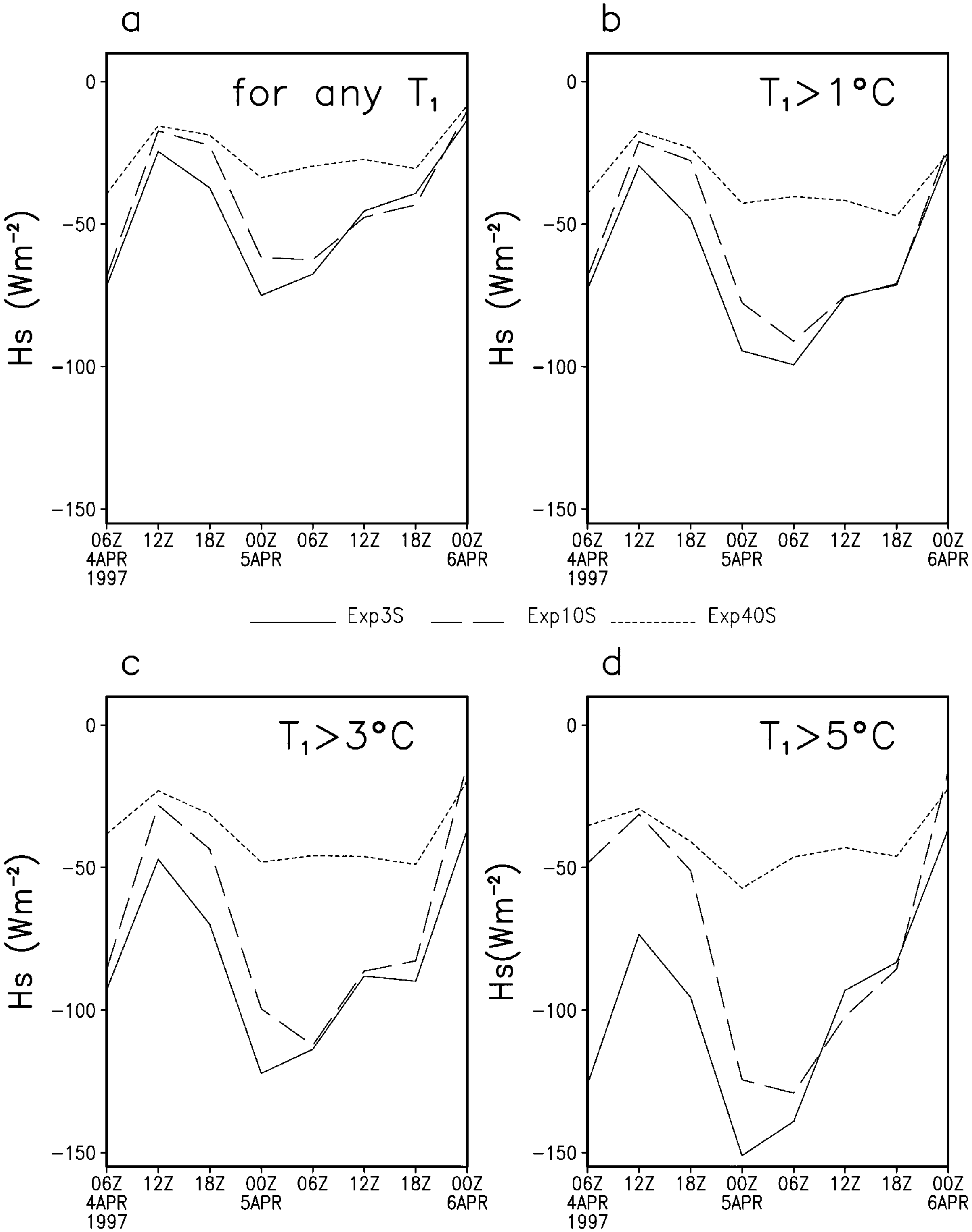

FIG. 8. As in Fig. 6, but for exp3S, exp10S, and exp40S.

In simulations of regional snowmelt under warm advection conditions there undoubtedly are a variety of uncertainties, particularly in initializing the snow layer and related physical surface characteristics. These uncertainties together with an incomplete model physical formulation (particularly in regional-scale models) are likely to produce biases in the predicted snowmelt. Although some model shortcomings are difficult to improve because of their complexity, inadequate observations, and other constraints, lowering the first model

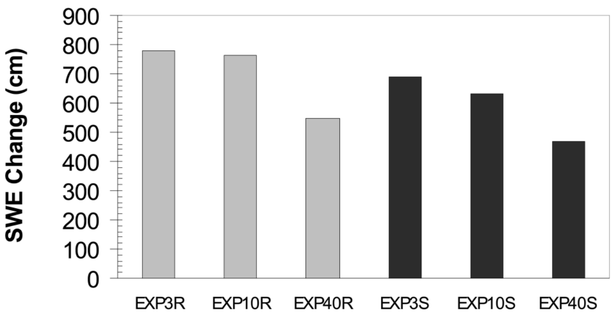

FIG. 9. Change in SWE summed over all initially snow-covered grid points during the 48-h period of 4–5 Apr 1997 for the indicated six simulations.

level as suggested in this paper can be implemented relatively easily. When the vertical eddy diffusion of momentum, temperature, and moisture is formulated numerically using an explicit time scheme, lowering the first model level may require reduction of the time step. However, many models adopt implicit numerical schemes for diffusion and are thus less sensitive to the selection of the time step (as long as complex terrain is not involved). The need to reduce the time step could be a computational disadvantage in a long climate simulation. However, for short-period simulation the time step reduction needed to simulate warm advection–related snowmelt is computationally insignificant.

Last, we note that results of this study may be extended to cases of simulated outbreaks of warm air masses over cooler water bodies or ice surfaces, as may occur in various geographical locations over the globe. In such situations the surface thermal fluxes typically are important, so that a relatively low first model level would be needed for simulating these situations, too.

Acknowledgments. The study was supported by NASA Grant NAG57561 and NSF Grant ATM9911417. The computations were carried out at the NCAR Climate Simulation Laboratory. This is Journal Paper J-19092 of the Iowa Agricultural and Home Economics Experiment Station, Ames, Iowa, Projects 3803 and 3435 and supported by the Hatch Act and State of Iowa. We thank Don Cline for providing us with his snow model output. Comments by reviewers of this paper improved its clarity. Reatha Diedrichs prepared the manuscript.

REFERENCES

Cline, D. W., 1997: Snow surface energy exchanges and snow melt at continental, midlatitude Alpine site. *Water Resour. Res.,* **33,** 689–701.

——, and T. R. Carroll, 1999: Inference of snow cover beneath obscuring clouds using optical remote sensing and a distributed snow energy and mass balance model. *J. Geophys. Res.,* **104,** 19 631–19 644.

Dudhia, J., 1989: Numerical study of convective observed during the winter monsoon experiment using a mesoscale two dimensional model. *J. Atmos. Sci.,* **46,** 3077–3107.

Grell, G. A., 1993: Prognostic evaluation of assumptions used by cumulus parameterizations. *Mon. Wea. Rev.,* **121,** 764–787.

——, J. Dudhia, and D. S. Stauffer, 1995: A description of the Fifth-Generation Penn State–NCAR Mesoscale Model (MM5). NCAR Tech. Note NCAR/TN-398+STR, 122 pp.

Kalnay, E., and Coauthors, 1996: The NCEP/NCAR 40-Year Reanalysis Project. *Bull. Amer. Meteor. Soc.,* **77,** 437–471.

Leathers, D. J., D. R. Kluck, and S. Kroczynski, 1998: The severe flooding event of January 1996 across north-central Pennsylvania. *Bull. Amer. Meteor. Soc.,* **79,** 785–797.

Moore, D. R., 1983: On the use of bulk aerodynamic formula over melting snow. *Nordic Hydrol.,* **14,** 193–206.

Panofsky, H. A., and J. A. Dutton, 1984: *Atmospheric Turbulence.* John Wiley and Sons, 397 pp.

Segal, M., J. R. Garratt, R. A. Pielke, P. Hildebrand, F. A. Rogers, J. Cramer, and A. Schanot, 1991: On the impact of snow cover on daytime pollution dispersion. *Atmos. Environ.,* **25B,** 177–192.

Skibin, D., and J. A. Businger, 1985: The vertical extent of the log-linear wind profile under stable stratification. *Atmos. Environ.,* **19,** 27–30.

Takle, E. S., and Coauthors, 1999: Project to Intercompare Regional Climate Simulations (PIRCS): Description and initial results. *J. Geophys. Res.,* **104,** 19 443–19 461.

Zhang, D.-L., and R. A. Anthes, 1982: A high-resolution model of the planetary boundary layer—sensitivity tests and comparisons with SESAME-79 data. *J. Appl. Meteor.,* **21,** 1594–1609.